Estimation of the wave-related ripple characteristics and induced bed shear stress

B. Camenen

▶ **To cite this version:**

B. Camenen. Estimation of the wave-related ripple characteristics and induced bed shear stress. Estuarine, Coastal and Shelf Science, 2009, 84 (4), p. 553 - p. 564. 10.1016/j.ecss.2009.07.022 . hal-00456157

HAL Id: hal-00456157
https://hal.science/hal-00456157

Submitted on 12 Feb 2010

HAL is a multi-disciplinary open access archive for the deposit and dissemination of scientific research documents, whether they are published or not. The documents may come from teaching and research institutions in France or abroad, or from public or private research centers.

L'archive ouverte pluridisciplinaire **HAL**, est destinée au dépôt et à la diffusion de documents scientifiques de niveau recherche, publiés ou non, émanant des établissements d'enseignement et de recherche français ou étrangers, des laboratoires publics ou privés.

Author-produced version of the article published in Estuarine Coastal and Shelf Science,
vol. 84, n° 4, p. 553-564, doi : 10.1016/j.ecss.2009.07.022

Estimation of the wave-related ripple characteristics and induced bed shear stress

Benoît Camenen

Cemagref, UR HHLY, 3 bis quai Chauveau, CP 220, F-69336 Lyon cedex 09, France
Email: benoit.camenen@cemagref.fr

Abstract

A large data set on ripples was collected and examined. A set of new formulas for the prediction of the ripple characteristics is proposed with an emphasis on the disappearance of the ripples. The ripple wavelength was observed to be proportional to the bottom wave excursion but also to be a function of the grain-related Shields parameter and wave period parameter introduced by Mogridge *et al.* (1994). The ripple steepness was found to be nearly constant for orbital ripples, and with a sharp decrease for suborbital ripples. Two empirical functions are added including the effects of the critical Shields parameters (inception of transport and inception of sheet flow), *i.e.* giving the boundaries for the ripple existence's domain. The proposed formulas yield better prediction capabilities compared to the previously published formulas, especially when ripples are washed out. The effect of the ripple characteristics on the roughness height and the calculation of the bed shear stress is also discussed. It appeared that the bed shear stress calculation is more sensitive to the empirical coefficient a_r introduced in the estimation of the ripple-induced roughness height or to the limits of existence of the ripples than the ripple characteristics themselves.

Keywords

wave ripples; ripple height; ripple steepness; roughness height; bed shear stress; predictive formula

1 Introduction

An important issue for the prediction of the suspended load in coastal waters is to estimate the bottom shear stress due the oscillatory movement of the waves. Close to the shore, the wave-related bed shear stress often prevails on the current-related bed shear stress, and thus significantly influences the estimation of the bottom reference concentration and sediment diffusivity, which are the main parameters for

Author-produced version of the article published in Estuarine Coastal and Shelf Science,
vol. 84, n° 4, p. 553-564, doi : 10.1016/j.ecss.2009.07.022

the suspended load (Camenen & Larson, 2008). When ripples appear, their effects on the roughness height and bottom shear stress are very significant (Van Rijn, 1993). Van der Werf *et al.* (2006) also showed the strong influence of ripples on the direction of the net suspended load, as they induce some phase-lag in the suspension concentration. It is then extremely important to predict correctly the characteristics of the ripples and induced roughness height.

Unlike current-related bed forms, wave ripples are generally symmetric with sharper crests due to the to and fro movement of wave orbital velocity. Bagnold (1946) called rolling-grain ripples the ripples first appearing on a flat bed exposed to wave-action. For this regime close to the inception of motion, the grains roll back and forth and form small triangular ridges. According to Bagnold (1946), these ripples are stable only if the shear stress stays close to its critical value for the inception of movement. If the flow magnitude increases, the lee-side vortex becomes strong enough to initiate grain motion in the space between the two ripples. The ripples grow until an equilibrium geometry corresponding to the so-called vortex ripples.

The ripple wave length L_r is often assumed to be proportional to the semi-excursion amplitude of orbital motion A_w: $1 < L_r/A_w < 2$. And the ripple wave steepness H_r/L_r (where H_r is the ripple height) varies from 0.1 (vortex formation) to 0.25 (slope stability). Wiberg & Harris (1994) made a very careful description of ripple characteristics. In their classification, ripples are subdivided into three groups: orbital, suborbital and anorbital. The basic scaling of orbital ripple wavelength is on A_w, whereas the basic scaling of anorbital ripples is on the median grain size d_{50}; suborbital ripples represent the transitional region between these two limits. Orbital ripples have an almost constant steepness of $H_r/L_r = 0.17$, while anorbital ripples are less steep, with a steepness decreasing as orbital diameter increases for a given grain size.

Recently, Hanes *et al.* (2001) observed in the field long-wave ripples (LWR) with relatively small heights (ranging from 3 mm to 6 cm) and large lengths (ranging from 35 to 200 cm). LWR were observed to be not as dynamics as the small-wave ripples (SWR) commonly observed. And they also observed some coexistence for both types of ripples. One explanation for LWR is that the peak frequency near the seabed may be different (smaller) than the peak frequency of the surface elevation because of the frequency-dependent reduction of fluid orbital amplitude with depth. Other assumptions for their origin may be a larger suspension within the boundary layer and a regime close to the sheet-flow regime (Hanes *et al.*, 2001). Kleinhans (2005) described them as skewed hummocks with much sediment suspension but no strong vortex shedding, associated with large orbital flows possibly combined with small currents.

For strong conditions (typically storm conditions), ripples are washed out. It corresponds to the inception of the sheet-flow regime where most of the sediment transport occurs in a thin layer close to the bed. This regime occurs when the Shields parameter, mobility parameter, orbital Reynolds number or the ratio $A_/d_{50}$ reach some critical value: $\theta_w > 0.8$, $\Psi_w > 100$, $\Re_w > 2 \times 10^6$ or $A_/d_{50} = 6000$ approximately (*cf.* Van Rijn, 1993 or Camenen & Larson, 2006) where the wave-

Author-produced version of the article published in Estuarine Coastal and Shelf Science,
vol. 84, n° 4, p. 553-564, doi : 10.1016/j.ecss.2009.07.022

related Shields parameter, mobility parameters, wave period parameter, and orbital Reynolds number are defined as follows:

$$\theta_w = \frac{0.5 f_w {U_w}^2}{(s-1) g d_{50}} \quad (1)$$

$$\Psi_w = \frac{{U_w}^2}{(s-1) g d_{50}} = \left[\frac{\pi A_w}{d_{50}}\right]^2 \chi \quad (2)$$

$$\chi = \frac{d_{50}}{(s-1) g {T_w}^2} \quad (3)$$

$$\Re_w = \frac{{U_w}^2}{\omega \nu} \quad (4)$$

with U_w the wave orbital velocity, s the relative sediment density, g the acceleration of gravity, f_w the wave-related friction factor, $A_w = U_w T_w/(2\pi)$ the wave orbital semi excursion, T_w the wave period, $\omega = 2\pi/T_w$, and ν the kinematic viscosity of water.

Many authors proposed empirical relationships to describe the ripple characteristics, based on the mobility parameter Ψ_w: Nielsen (1981), Wikramanayake & Madsen (1991), Van Rijn (1993), or Grasmeijer & Kleinhans (2004); on the Shields parameter θ_w: Grant & Madsen (1982); on the wave period parameter χ: Mogridge *et al.* (1994); on the ratio A_w/d_{50}: Wiberg & Harris (1994) or Soulsby & Whitehouse (2005 and 2007**?**); or on the orbital Reynolds number: Williams *et al.* (2005). These equations are presented in detail in appendix. Most of these formulas are however only based on experimental data where ripples exist. In order to properly estimate the total shear stress, it is also fundamental to validate these formulas over plane beds when the ripples are washed out. For random waves, authors usually suggested to use the significant wave characteristics for the prediction. Then, most of the formulas are assumed valid for both monochromatic and random waves.

The main purpose of this study is to provide a formula which correctly predicts ripple characteristics but also ripple disappearance in order to estimate properly the total bed shear stress for any wave condition. This paper is organized as follows: The experimental data used for this study are described and compared with the studied formulas. New formulas for the prediction of the ripple characteristics and their validation are presented next. Then, a presentation of the computation of the total shear stress is made as well as a sensitivity analysis on the main parameters. Finally, conclusions concerning the validity of the formulas and a discussion on the calculation of the total shear stress in the nearshore are also provided.

2 On the prediction of ripple characteristics

2.1 Experimental data

In order to compare the results obtained using empirical formulas with experimental data, several data sets were compiled. In Tab. 1, the main hydrodynamic and sedimentologic parameters are presented, as well as the type of the experiment.

Author-produced version of the article published in Estuarine Coastal and Shelf Science,
vol. 84, n° 4, p. 553-564, doi : 10.1016/j.ecss.2009.07.022

Table 1: Data summary for experiments on ripple characteristics.

Author(s)	Name	**Location**	**Flow Type**	**nbr. exp.**	d_{50} $[mm]$	h $[m]$	U_c $[m/s]$	U_w $[m/s]$	T_w $[s]$	H_r $[cm]$	L_r $[cm]$
Inman (1957)	Inm57	US Corps of Engineers, USA	field	41	0.1-0.9	0.5-2.0	-	0.06-0.57	5.0-13	0.5-19	6-105
Lofquist (1978)	Lof78	US Corps of Engineers, USA	oscillatory flow tunnel	13	0.18-0.26	0.4	0	0.41-1.22	2.7-15	0-19	11-120
Sleath (1982)	Sle02	Cambridge University, United Kingdom	oscillatory flow tunnel	13	0.20, 0.41	0.15	0	0.16-0.44	2.9-5.1	2-5	12-32
Bosman (1982) and Steetzel (1985)	DLL80s	DHL, Delft, The Netherlands	wave flume	70	0.10	0.1-0.65	0.10-0.32	0.13-0.30	1.4-2.0	1-3	8
Sato (1987)	Sat87	Tokyo University, Japan	oscillatory flow tunnel	66	0.18	0.21	0	0.11-0.65	0.5-7.0	0-3	0-18
Ribberink & Al Salem (1994)	Rib90s	DHL, Delft, The Netherlands	large water tunnel	71	0.21	0.8	0	0.2-1.5	2.0-12.0	0-35	0-300
Van Rijn *et al.* (1993)	VR93	Delft Univ., The Netherlands	wave flume	45	0.1-0.22	0.48-0.52	−0.45-0.45	0.14-0.39	2.2-2.7	0.6-2.9	6-20
Van Rijn & Havinga (1995)	VRH95	DHL, Delft, The Netherlands	wave basin	28	0.1	0.40-0.43	0-0.32	0.14-0.30	2.1-2.3	0.6-1.4	6-11
Hume *et al.* (1999)	Hum99	NIWA, USA	field	9	0.4	25	-	0.28-1.06	11.0	3-13	40-90
Khelifa & Ouellet (2000)	KO00	Laval, Canada	wave basin	48	0.15-0.5	0.3	0-0.34	0.08-0.26	0.9-1.4	0.4-1.7	3-12
Doucette (2000, 2002)	Dou02	Various beaches, Australia	field	84	0.14-0.62	0.18-1.73	-	0.15-1.00	2.2-12.2	0-14	0-91
SEDMOC data set (2001)	TUF80s	Grote Speurwerk (35m), DUT, Delft, The Netherlands	wave flume	125	0.10-0.22	0.29-0.60	0.07-0.45	0.17-0.55	1.2-2.7	0.2-2.9	0.6-20
O'Donoghue & Clubb (2001)	oDC01	Aberdeen University, United Kingdom	flow tunnel	35	0.18-0.44	0.75	0	0.25-0.94	2.0-15	0.9-19	6-121
Hanes *et al.* (2001)	Han01	Duck, North Carolina, USA	field	201	0.12-1.7	1.4-7	-	0.12-1.62	3.1-16	0-13	0-270
Sleath & Wallbridge (2002)	Sle02	Cambridge University, United Kingdom	oscillatory flow tunnel	29	0.20-0.80	0.15	0	0.12-1.64	2.8-6.8	0-9	0-50
Faraci & Foti (2002)	FF02	Catania University, Italy	wave flume	38	0.25	0.29	-	0.12-0.35	1.2-4.2	0.7-2.1	4-11
Delgado Blanco *et al.* (2004)	Del04	Deltaflume, Delft, The Netherlands	large wave flume	17	0.18-0.44	7.0	0	0.14-0.74	6	0.6-5	10-35
Van der Werf & Ribberink (2004)	vdWR04	DHL, Delft, The Netherlands	large water tunnel	10	0.35	0.8	0	0.42-0.85	5.0-10.0	2.5-13.9	44-113
Grasmeijer & Kleinhans (2004)	GK04	Egmond aan Zee, The Netherlands	field	45	0.24	1.5-5.0	−0.40-0.10	0.23-0.99	4.0-10.5	0.7-10	19-200
Williams *et al.* (2004)	Wil04	Deltaflume, Delft, The Netherlands	large wave flume	65	0.16-0.35	4.0-4.5	0	0.13-1.03	4.0-6.0	0.3-7	20-104
Catano-Lopera & Garcia (2006a, b)	Cat06	University of Illinois, USA	wave flume	23	0.25	0.36-0.76	0-0.6	0.25-0.42	2.0-6.9	1.5-3.5	9.1-18.8

Author-produced version of the article published in Estuarine Coastal and Shelf Science,
vol. 84, n° 4, p. 553-564, doi : 10.1016/j.ecss.2009.07.022

For all the experiments presented in Tab. 1, sand with a relative density $s = 2.65$ was used. Several of these data sets were obtained from the data compilation provided by the SEDMOC (2001) European Union research project.

2.2 Comparison between experimental data and empirical relationships for ripple characteristics

A comparison between the experimental data and the empirical relationships presented previously was undertaken. Tab. 2 summarizes the results obtained for the prediction of the ripple height and length where $P2$ and $P5$ indicate the percentage of data correctly predicted within a factor 2 or 5, respectively. The mean value (μ_f) and standard deviation (σ_f) of the function $f(X) = \log|X_{pred}/X_{meas}|$ is also presented, where X_{pred} and X_{meas} are the predicted and measured values (H_r or L_r), respectively. To avoid zero-values in the experimental data or predicted data, a minimum value for H_r and L_r was assumed (equal to $2d_{50}$ and $10d_{50}$, respectively). The Williams *et al.* (2005) formulas were proposed for suborbital ripples only and thus are valid for large values of the ratio A_w/d_{50} only. Because of its obvious limits, this formula will not be used in the following study.

Table 2: Prediction of the ripple characteristics using various empirical equations and the collected experimental data with purely oscillatory flows.

	ripple length L_r				ripple height H_r			
Equation	$P2$	$P5$	μ_f	σ_f	$P2$	$P5$	μ_f	σ_f
Nielsen	35%	61%	−0.11	0.84	35%	60%	−0.34	0.79
Grant & Madsen	59%	76%	+0.36	0.99	44%	71%	+0.17	0.85
Wikramanayake & Madsen	45%	75%	+0.04	0.81	37%	67%	−0.09	0.74
Van Rijn	61%	80%	+0.10	0.84	56%	78%	+0.02	0.79
Mogridge *et al.*	62%	82%	+0.36	0.78	45%	71%	+0.63	0.82
Wiberg & Harris	54%	82%	+0.09	0.76	55%	82%	+0.15	0.66
Grasmeijer & Kleinhans	58%	81%	+0.26	0.89	39%	74%	+0.02	0.74
Soulsby & Whitehouse	66%	79%	+0.19	0.80	65%	84%	+0.06	0.63
Eqs. 9 and 10 with $\alpha_{cr} = 0.01$	66%	81%	+0.17	0.76	68%	88%	−0.05	0.56
Eqs. 9 and 10 with $\alpha_{cr} = 1$	64%	80%	+0.02	0.83	65%	84%	−0.14	0.64

For the prediction of the ripple length, it appears that the Grant & Madsen, Mogridge *et al.*, Van Rijn, Wiberg & Harris, Grasmeijer & Kleinhans formulas and more especially the Soulsby & Whitehouse formula yield the best results. For the prediction of the ripple height (which is actually dependent on the prediction of the ripple length), the Van Rijn, Wiberg & Harris, and Soulsby & Whitehouse formulas yield the best results. Apart from the Nielsen and Wikramanayake & Madsen formulas, all formulas tend to generally overestimate measured ripple height and length. The Wiberg & Harris and Mogridge *et al.* formulas yield smaller dispersion

for the ripple height prediction compared to the Grant & Madsen, Soulsby & Whitehouse and Van Rijn formulas. This may be partly explained as former formulas do not take into account the critical Shields parameters for the presence of ripples. As the comparison is made with data where ripples exist, a model that predicts the absence of ripple would yield significant underestimation. It is particularly significant for the effect of θ_{cr} as several data indicate the occurrence of ripples whereas the Shields parameter is smaller than θ_{cr} (estimated in this paper using Eq. 5). Actually, as noted by Soulsby & Whitehouse (2007**?**), when $\theta_w \leq \theta_{cr}$, ripples should take pre-existing values of H_r and L_r, which are not necessarily null. However, in nature, there are many cases where the bed is flat. Even if some uncertainties exist on the prediction on the critical Shields parameters (inception of sediment movement or sheet flow), it is very important to be able to predict the appearance and disappearance of ripples and not to overestimate the roughness height when the bed is flat. The Nielsen, Van Rijn and Grasmeijer & Kleinhans formulas give a sheet flow threshold for $(\theta_w)_{cr,sf} = 1$ or $(\Psi_w)_{cr,sf} = 250$ or 156, respectively. Another remark is that the Wiberg & Harris and Soulsby & Whitehouse formulas predict a nearly constant value for the ratio $H_r/L_r \approx 0.15$ when $A_w/d_{50} < 1000$ and a rapid decrease in steepness when $A_w/d_{50} > 3000$. For these two formulas, the threshold of sheet-flow is described in term of A_w/d_{50} ($(A_w/d_{50})_{cr,sf} \approx 6000$, which seems to be too large, see section 3.1). As a conclusion, the Soulsby & Whitehouse formula yields the best prediction for the estimation of the ripple characteristics using the collected data; the Van Rijn formula yields a lower score for the prediction but it seems to better take into account the effect of the threshold for the inception of sheet flow.

2.3 Capabilities of the various formulas to predict the absence of ripples

To confirm these observations, a comparison is provided using data for the inception of sheet flow (*cf.* Sec. 3.1 and Camenen & Larson, 2006). When the sheet flow regime just appears, the bed is flat and the roughness height may be assumed to be equal to the grain-related roughness, *i.e.* $k_s = k_{sg} = 2d_{50}$. In Tab. 3, the "measured" (assuming $k_s = k_{sg}$) and "estimated" (based on the estimated ripple characteristics and using Eq. 17) roughness heights are compared.

The results from Tab. 3 clearly indicates the weakness of most of the predictive formulas. As they are based and fitted on experimental data where ripples exist, they do not forecast properly the absence of ripple. Only the Nielsen, Van Rijn and the Grasmeijer & Kleinhans formulas predict a disappearance of the ripples even if some large uncertainties are encountered to predict this limit. The Nielsen formulas yield the best results just because it tends to underestimate $\theta_{cr,sf}$.

Author-produced version of the article published in Estuarine Coastal and Shelf Science,
vol. 84, n° 4, p. 553-564, doi : 10.1016/j.ecss.2009.07.022

Table 3: Prediction of the roughness height when the ripples are washed out and the sheet flow regime reached.

Equation	$P2$	$P5$	μ_f	σ_f
Nielsen	87%	97%	+0.10	0.20
Grant & Madsen	20%	41%	+0.80	0.47
Wikramanayake & Madsen	13%	31%	+1.13	0.62
Van Rijn	41%	57%	+0.56	0.52
Mogridge *et al.*	1%	18%	+1.10	0.43
Wiberg & Harris	0%	0%	+1.68	0.39
Grasmeijer & Kleinhans	24%	78%	+0.51	0.26
Soulsby & Whitehouse	0%	0%	+1.71	0.33
Eqs. 9 and 10, $\alpha_{cr} = 0.01$	4%	4%	+1.57	0.40
Eqs. 9 and 10, $\alpha_{cr} = 1$	47%	55%	+0.63	0.65

3 A new model for the calculation of the ripple characteristics

3.1 Limits for the ripple existence

A need clearly comes out from the above study for the estimation of the ripple characteristics, which is to estimate carefully their limits of existence, *i.e.* the critical Shields parameters corresponding to their appearance and disappearance. As concerns the appearance of ripples, it may be assumed that they exist as soon as sediments move. The critical Shields parameter for the inception of movement may be estimated using the equation proposed by Soulsby & Whitehouse (1997),

$$\theta_{cr} = \frac{0.30}{1 + 1.2 d_*} + 0.055 \ [1 - \exp(-0.02 d_*)] \tag{5}$$

where $d_* = [g(s-1)/\nu^2]^{1/3} d_{50}$ is the dimensionless grain size.

Camenen & Larson (2006) proposed a maximum value of the wave orbital velocity $U_{w,cr,sf}$ for the inception of the sheet flow regime or wash-out of the wave ripples,

$$U_{w,cr,sf} = 8.35 \sqrt{(s-1) g \sqrt{d_{50} \ \delta_w}} \ (1 + r_w) \tag{6}$$

where $\delta_w = \sqrt{\nu T_w / \pi}$ is the thickness of the Stokes boundary layer and r_w the wave asymmetry ($r_w = (u_{w,max} - u_{w,min}/(u_{w,max} + u_{w,min})$ with $u_{w,max}$ and $u_{w,min}$ are the maximum onshore and minimum offshore velocity, respectively). A simple empirical equation has been suggested by Hanson & Camenen (2007) for the wave induced friction factor (validated with plane bed data), which may be written as follows:

$$f_w = \frac{0.5}{\sqrt{\pi}} \ {d_*}^{-3/4} \ \frac{d_{50}}{\delta_w} \tag{7}$$

Author-produced version of the article published in Estuarine Coastal and Shelf Science,
vol. 84, n° 4, p. 553-564, doi : 10.1016/j.ecss.2009.07.022

Thus, an expression for the critical Shields parameter $\theta_{cr,sf}$ for the inception of sheet-flow may be obtained from Eqs. 1, 6 and 7:

$$\theta_{cr,sf} = 10\ {d_*}^{-3/4} \sqrt{\frac{d_{50}}{\delta_w}}\ (1 + r_w)^2 \tag{8}$$

Using the same experimental data as Camenen & Larson (2006), Eq. 8 shows relatively good results (*cf.* Fig. 1). It can also be observed from the data that the critical Shields parameter for the inception of sheet flow may vary from 0.2 to 2.0.

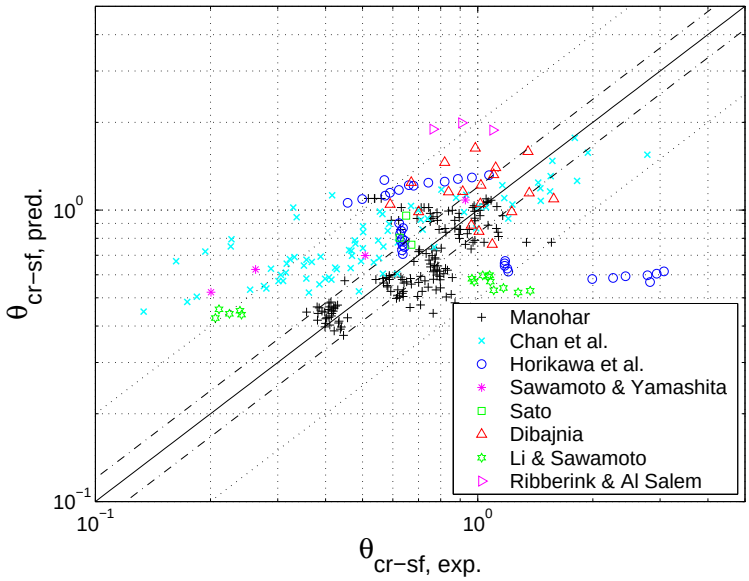

Figure 1: Estimation of the critical Shields parameter for the inception of wave-related sheet flow using Eq. 8.

It should be noted that the threshold of sheet-flow in term of $(A_w/d_{50})_{cr,sf}$ (as used by Wiberg & Harris, 1994, or Soulsby & Whitehouse, 2005) varies from 60 to 6000 using the same experimental data as Camenen & Larson (2006). Thus, the Wiberg & Harris and Soulsby & Whitehouse formulas seem to overestimate this threshold as they assume $(A_w/d_{50})_{cr,sf} \approx 6000$.

3.2 New equations for the description of the ripple characteristics

Following the previous observations, two simple equations function of the skin Shields parameter and its critical values only (inception of movement and inception of sheet flow) are proposed to predict the ripple length and steepness, respectively:

$$\frac{L_r}{A_w} = \left(\frac{L_r}{A_w}\right)_{eq} f\left(\frac{\theta_{cr}}{\theta_{wg}}\right)\ f\left(\frac{\theta_{wg}}{\theta_{cr,sf}}\right) \tag{9}$$

$$\frac{H_r}{L_r} = \left(\frac{H_r}{L_r}\right)_{eq} f\left(\frac{\theta_{cr}}{\theta_{wg}}\right)\ f\left(\frac{\theta_{wg}}{\theta_{cr,sf}}\right) \tag{10}$$

where the subscript eq corresponds to the equilibrium value of the ratio L_r/A_w and H_r/L_r, respectively, θ_{wg} is the grain-related Shields parameter (computed assuming $k_s = 2d_{50}$) and f is a function defining the existence of the ripples or not:

$$f(x) = \exp\left(-\alpha_{cr} x^4\right) \tag{11}$$

with α_{cr} a coefficient.

Grant & Madsen (1982), Van Rijn (1993) or Grasmeijer & Kleinhans (2004) observed that $(L_r/A_w)_{eq}$ is a decreasing function of Ψ_w or θ_w. On the other hand, Mogridge *et al.* (1994) found a relationship between the ratio L_r/d_{50} and the wave period parameter χ. In Fig. 2, the ripple wavelength normalised by the wave orbital semi-excursion L_r/A_w was plotted against the grain-related Shields parameter θ_{wg} with the wave period parameter χ emphasised (for practical purpose, flat beds are represented in this figure by the value $L_r/A_w = 10^{-2}$). It appears that the ratio L_r/A_w does decrease with the grain-related Shields parameter θ_{wg} but with a varying slope that depends on χ. A relationship for the equilibrium value of the ratio L_r/A_w is suggested as a function of θ_{wg} and χ:

$$\left(\frac{L_r}{A_w}\right)_{eq} = 1.6\ \exp(-5\times10^{-3}\ \chi^{-0.4})\ {\theta_{wg}}^{-0.025\chi^{-0.2}} \tag{12}$$

Some uncertainties obviously exist in the determination of the critical Shields parameter for the inception of sheet flow. Indeed, many data from Hanes *et al.* indicate a disappearance of ripples for much smaller Shields parameter than expected. Unlike the observations by Wiberg & Harris (1994), the collected data do not show any clear relationship between the ripple length and the grain size (when $A_w > 3000$) corresponding to the anorbital ripples. Only orbital and suborbital ripples were observed. It should also be noted that there is a relationship between χ and Eq. 8 for $\theta_{cr,sf}$, and $\chi = 10^{-8}\pi^{-2}{\theta_{cr,sf}}^8 {d_*}^3$.

The ripple steepness was often observed to be nearly constant, and $H_r/L_r \approx 0.16$ (Wiberg & Harris, 1994). As observed by Soulsby & Whitehouse (2005), the ripple steepness appears to be strongly dependent on the ratio A_w/d_{50} with a smaller steepness for suborbital ripples ($A_w/d_{50} > 1000$). In Fig. 3, the ripple steepness H_r/L_r was plotted against wave orbital semi-excursion normalised by the median grain size A_w/d_{50} with the wave period parameter emphasised. A clear decrease of the ripple steepness with the ratio A_w/d_{50} may be observed. The following equation for the equilibrium ripple steepness is then suggested,

$$\left(\frac{H_r}{L_r}\right)_{eq} = 0.16\ \exp\left[-1.0\times10^{-7}\ \left(\frac{A_w}{d_{50}}\right)^2\right] \tag{13}$$

The introduction of the function f in Eqs. 9 and 10 was proposed to properly evaluate the non-existence of the ripples. As some uncertainties exist on the prediction of θ_{cr} or $\theta_{cr,sf}$, this exponential function allows positive values for H_r and L_r, but much smaller than their equilibrium values.

In Fig. 4, Eqs. 9 and 10 are plotted versus the grain-related Shields parameter for four values of the critical Shields parameter for the inception of sheet flow

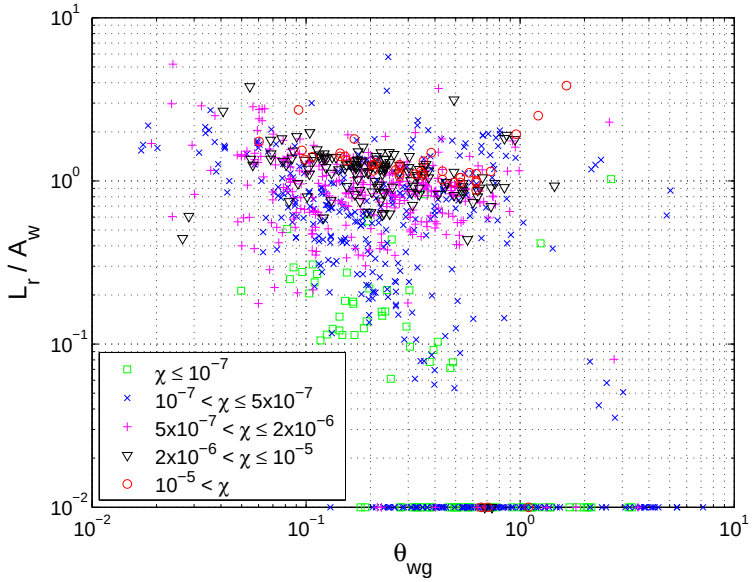

Figure 2: Wave-generated ripple wavelength normalised by the wave orbital semi-excursion as a function of the grain-related Shields parameter with the wave period parameter emphasised.

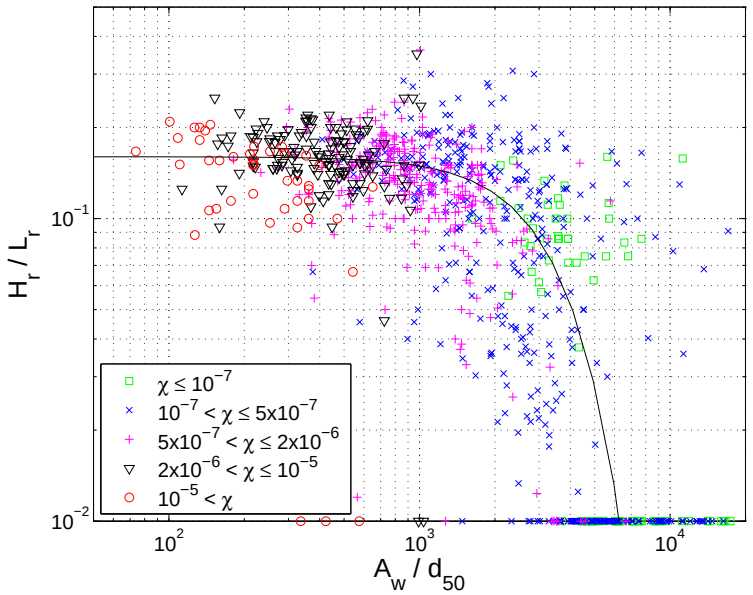

Figure 3: Wave-generated ripple steepness as a function of the wave orbital semi-excursion normalised by the median grain size with the wave period parameter emphasised (the solid line corresponds to Eq. 13).

($\theta_{cr,sf}$ =0.75, 1.0, 1.25 and 1.5) for a given grain size (d_{50} = 0.3 mm). The wave period is estimated using the relationship between χ and Eq. 8 for $\theta_{cr,sf}$. As expected, the proposed formulas yield a ripple steepness which depends mainly on the ratio $\theta_{wg}/\theta_{cr,sf}$ and a slightly more complex function for the ratio H_r/A_w. Compar-

ing with the experimental data (*cf.* Fig. 2), it appears that Eqs. 9, 10, 11 (with $\alpha_{cr} = 1$), 12, and 13, provide a good overview of the experimental data as soon as the critical Shields parameter for the inception of sheet flow is properly estimated. When $\theta_{cr,sf} < 0.8$ (or $\chi < 10^{-7}$), ripples present much smaller height and steepness or even may not occur whatever the Shields parameter.

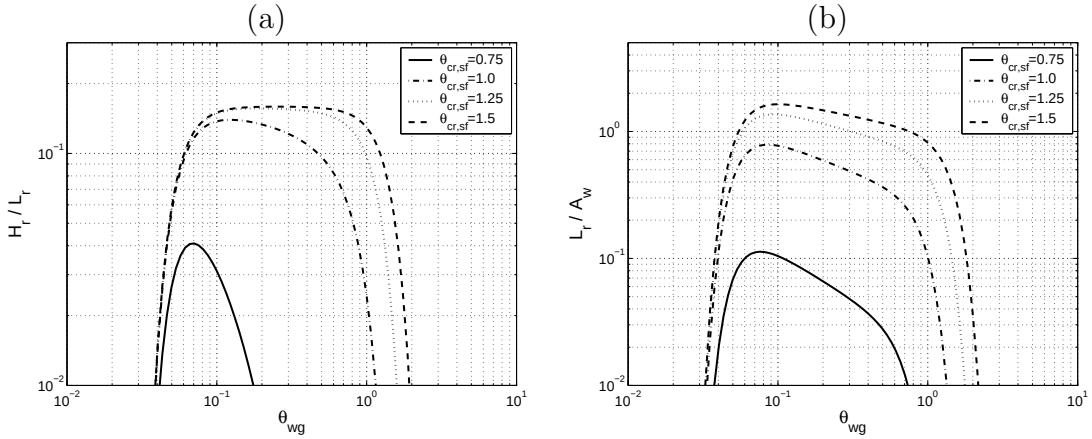

Figure 4: Ripple steepness H_r/L_r (a) and ratio L_r/A_w (b) versus the skin Shields parameter for several values of the critical Shields parameter for the inception of sheet flow $\theta_{cr,sf}$ using Eqs. 9 and 10 with $\alpha_{cr} = 1$ and $d_{50} = 0.3$ mm.

Using Eqs. 5 and 8 for the estimation of the different critical Shields parameter, Eqs. 9 and 10 yield good results for the prediction of the ripple characteristics (see Tab. 2). Of course, even if a large data set has been used, these good results (compared to the other formulas) are slightly biased as the newly proposed formulas were optimized using this data set. As shown in Tab. 3, the correct prediction of $\theta_{cr,sf}$ and its integration in the ripple formulas are fundamental not to overestimate largely the roughness (and thus the Shields parameter) when the ripples are washed out. The influence of the coefficient α_{cr} in Eq. 11 appears to be significant when sheet flow regime is reached. Indeed, if the choice of $\alpha_{cr} = 0.01$ or 1 does not affect significantly the results for the prediction of the ripple characteristics (results slightly poorer when $\alpha_{cr} = 1$, see Tab. 2), the choice of $\alpha_{cr} = 1$ seems much more appropriate to predict the absence of ripples (*cf.* Tab. 3).

3.3 Large wave ripples

For large wave ripples (LWR), all the proposed formulas overestimate the ripple height and steepness. In Fig. 5, the wavelength and steepness with LWR data from Hume *et al.* (1999) and Hanes *et al.* (2001) have been plotted against the grain-related Shields parameter. Compared to Eqs. 9 and 10, the behaviour against θ_{wg} seems to be properly reproduced (decrease of L_r/A_w with an increasing θ_{wg}). However, the ripple wavelength is underestimated by a factor 4 to 8. Apart from the data by Hume *et al.*, the wave steepness is also underestimated by a factor 4 to 8, which means that the ripple height is properly estimated. Thus, some LWR

could correspond to a more complex energetic system at the boundary layer where several frequencies coexist due to the frequency-dependent reduction of fluid orbital amplitude with depth. A higher frequency may control the ripple height whereas the smaller frequency may control the ripple length. Another hypothesis for the occurrence of the LWR is the relict (or fossil) ripples built during a previous event that may affect the ripple characteristics during the following period.

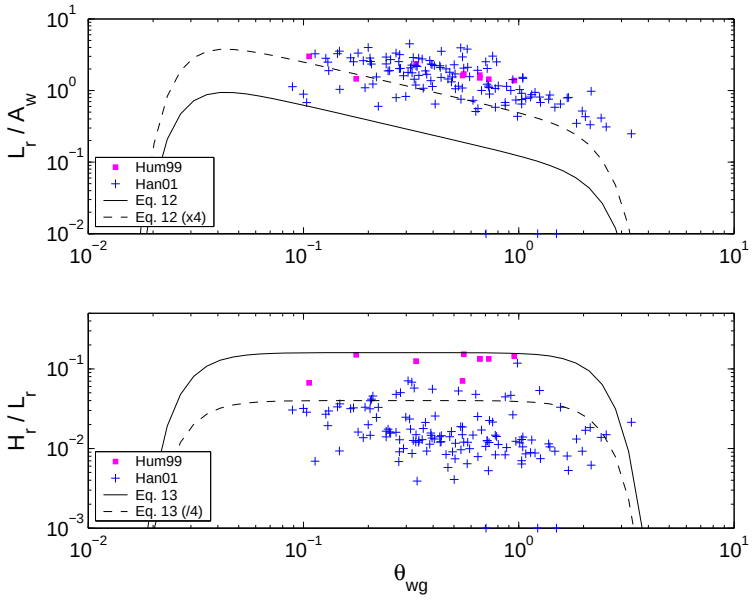

Figure 5: Large wave ripple (LWR) wavelength (normalised by the wave orbital semi-excursion) and steepness as a function of the grain-related Shields parameter.

3.4 Effects of a steady current

When a current was superimposed on the waves, Van Rijn *et al.* (1993) observed that ripples become asymmetrical and rapidly three-dimensional with increasing current. Khelifa & Ouellet (2000) showed that positive and negative longitudinal current velocities produce a similar effect on the ripple characteristics, *i.e.* an increase of the ripple length and height with increasing current. Based on kinetic considerations, they suggested to use the effective fluid orbital semi-excursion instead of the wave orbital semi-excursion,

$$\begin{aligned} A_{cw} &= \sqrt{{A_w}^2 + \left(\frac{T_w U_c}{2}\right)^2 + A_w T_w |U_c| |\cos\phi|} \\ &= A_w \sqrt{1 + \left(\frac{\pi U_c}{U_w}\right)^2 + 2\pi \frac{|U_c|}{U_w} |\cos\phi|} \end{aligned} \tag{14}$$

where U_c is the steady current and ϕ the angle between the wave and current directions. Following this idea, the Shields parameter in a wave and current interaction

may be estimated such as $\theta_{cw} = \theta_w(A_{cw}/A_w)^2$. It is thus possible to use Eqs. 9 to 13 in case of a wave and current interaction by replacing A_w and θ_w by A_{cw} and θ_{cw}, respectively.

In Fig. 6, the ratio between the predicted (using Eqs. 9 to 13) and measured ripple length and height is plotted versus the ratio $|U_c|/U_w$. It appears that, if both ripple length an height are properly estimated when $U_c = 0$, a significant over-estimation exists as soon as $|U_c|/U_w > 10^{-2}$ (where $L_{r,pred}/L_{r,meas} \approx 2$). No explanation was found to explain this reduction in the ripple dimensions due to a relatively low current. The change from 2D symmetrical ripples to 3D asymmetrical ripples may affect the average ripple length and height. When $|U_c|/U_w > 10^{-2}$, ripple characteristics are increasing as predicted by Eq. 14. As observed by Van Rijn & Havinga (1995), the angle between the wave and current directions has no significant influence on the ripple dimensions.

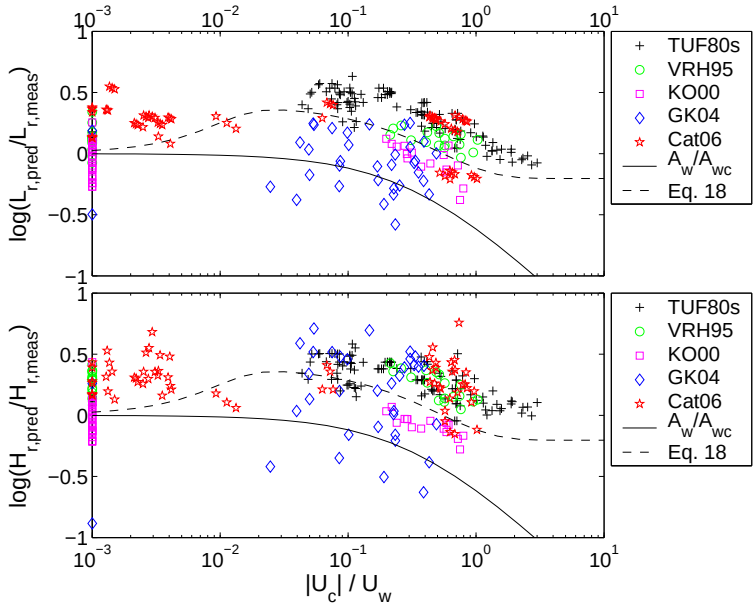

Figure 6: Prediction of the ripple wavelength and steepness using Eqs. 9 and 10 as a function of the ratio between the steady current amplitude of the wave orbital velocity.

As the steady current appears to induce two opposite effects on the ripple dimensions (decreasing when $|U_c|/U_w < 3 \times 10^{-2}$ and increasing $|U_c|/U_w > 3 \times 10^{-2}$), Eqs. 9 to 13 for waves alone still yield correct results (*cf.* Tab. 4). Using Eq. 14 improves the behaviour of the prediction against the ratio $|U_c|/U_w$. However, it tends to overestimate ripple dimensions; and the critical Shields parameter for inception of sheet flow is reached more easily (as $\theta_{cw} > \theta_w$), which yields a too fast disappearance of the ripples. An empirical coefficient for Eqs. 9 and 10 is suggested to improve the prediction of the ripple characteristics under waves and current:

$$r_{wc} = \left[1 - 0.6 \tanh\left(50\frac{|U_c|}{U_w}\right)\right]\left[1 + 3\tanh\left(\frac{|U_c|}{U_w}\right)\right] \tag{15}$$

As observed in Tab. 4, Eq. 15 significantly improves the results for the ripple prediction in case of a wave and current interaction.

Table 4: Prediction of the ripple characteristic under waves and current.

	ripple length L_r				ripple height H_r			
Equation	$P2$	$P5$	μ_f	σ_f	$P2$	$P5$	μ_f	σ_f
Eqs. 9 to 13	69%	100%	+0.16	0.24	59%	98%	+0.21	0.24
Eqs. 9 to 13 using Eq. 14	45%	95%	+0.16	0.52	50%	91%	−0.08	1.15
Eqs. 9 to 13 using Eq. 15	81%	99%	+0.08	0.23	73%	98%	+0.14	0.24

4 Estimation of the wave-related Shields parameter in case of ripples

The calculation of the bed shear stress in the nearshore is not trivial. The main difficulty lies in the determination of the wave-related friction factor f_w. f_w was calculated using the Swart formula (1974):

$$f_w = \min\left\{\exp\left[-6.0 + 5.2\left(\frac{A_w}{k_s}\right)^{-0.19}\right], 0.3\right\} \tag{16}$$

where the roughness height k_s needs to be estimated. Many uncertainties are then combined: they stem from the prediction of ripple characteristics but also their effects on the bed shear stress and the limits for the presence of ripples.

4.1 Calculation of the roughness height for a rippled bed

In the off-shore region where the ripples are generally observed, the shear stress due to the current is often much smaller than the shear stress due to the waves, and then, may be neglected in this study. The total roughness height k_s was estimated using the method proposed by Soulsby (1997) by summing the grain-related $k_{sg} \approx 2d_{50}$, form-drag k_{sf}, and sediment transport k_{ss} components, respectively: $k_s = k_{sg} + k_{sf} + k_{ss}$. When sheet flow regime occurs, the Wilson (1989) formula was used, *i.e.* $k_{ss} = 5\theta_w d_{50}$. Thereafter, the grain related Shields parameter θ_{wg} based on k_{sg} will be distinguished from the total Shields parameter θ_w based on k_s.

The ripple-related roughness height k_{sf} is generally calculated using the following formula,

$$k_{sf} = a_r \frac{{H_r}^2}{L_r} \tag{17}$$

where a_r is a constant ($5 < a_r < 40$). Nielsen (1992) suggested $a_r = 8$ whereas Van Rijn (1993) proposed $a_r = 20$.

Author-produced version of the article published in Estuarine Coastal and Shelf Science,
vol. 84, n° 4, p. 553-564, doi : 10.1016/j.ecss.2009.07.022

More recently, Kim (2004) investigated the effective form roughness of the wave ripples using a numerical model with a mixing length hypothesis to simulate the wave boundary layer flow over ripples. He obtained the ripple-length average bed shear stress (or form drag friction) from integration of the computed pressure field. An interesting conclusion from his study is that the effective roughness for sharp-crested ripples becomes about three times larger than that for the sinusoidal shape. It means that the presence of a steady current may considerably modify (reduce) the effective roughness as it will smooth the ripple crests. Nevertheless, this effect will be neglected in this study but may partly explain the different values suggested for a_r. Another explanation is the choice of the formula for f_w, which may influence afterwards the choice for a_r.

The ratio ${H_r}^2/L_r$ appeared to be a fundamental parameter for the estimation of the roughness height in the ripple regime, and thus for the estimation of the total Shields parameter. In Fig. 7(a), the ratio ${H_r}^2/L_r$ is plotted versus the ratio A_w/d_{50} using all the different studied formulas (assigned with initials of the authors or with the three first letters of the first author): The Nielsen (1981, Nie), Grant & Madsen (1982, GM), Wikramanayake & Madsen (1991, WM), Van Rijn (1993, VR), Mogridge *et al.* (1994, Mog), Wiberg & Harris (1994, WH), Grasmeijer & Kleinhans (2004, GK), Soulsby & Whitehouse (2005, SW), and Williams *et al.* (2005, Wil) formulas. As most beaches consist of sand with a grain size ranging from $d_{50} = 0.15$ to 0.35 mm, and because the wave period does not vary on a cross-shore profile (if the energy transfer to nearly harmonic wave components is neglected), this sensitivity analysis is presented for a varying wave excursion only, assuming a constant median grain size $d_{50} = 0.25$ mm and a constant wave period $T_w = 6$ s. It should be noted that the calculated values for ${H_r}^2/L_r$ do vary significantly depending on the fixed parameters (d_{50} or T_w). For the Soulsby & Whitehouse formula, $U_{1/10}$ was used instead of $U_{1/3}$ to represent the wave orbital velocity in case of irregular waves. When applied to regular waves, the curve should then be shifted rightward relative to the other curves.

Even if large discrepancies are observed between the different formulas, a similar trend for the coefficient ${H_r}^2/L_r$ may be observed:

- for $A_w/d_{50} < 1000$ (orbital ripples), ${H_r}^2/L_r$ is an increasing function of A_w/d_{50}.
- when $1000 < A_w/d_{50} < 3000$ (suborbital ripples), ${H_r}^2/L_r$ reaches a maximum which is similar whatever the formula, and then decreases. $({H_r}^2/L_r)_{eq} \approx 6 \times 10^{-3}$. This value appeared to be an increasing function of d_{50} or T_w.
- for $A_w/d_{50} > 3000$ (anorbital ripples), ${H_r}^2/L_r$ decreases rapidly toward zero.

It is also in accordance with Van Rijn (2007), who suggested a constant value for the ripple induced roughness height $k_{sf} = 150 d_{50}$ when $\Psi_w < 50$ with a quick decrease afterwards. Then, the main differences observed between the formulas are not in the magnitude of the coefficient ${H_r}^2/L_r$ but in the limits for the ripple presence (critical Shields parameters for the inception of movement and inception of sheet-flow, respectively).

Author-produced version of the article published in Estuarine Coastal and Shelf Science,
vol. 84, n° 4, p. 553-564, doi : 10.1016/j.ecss.2009.07.022

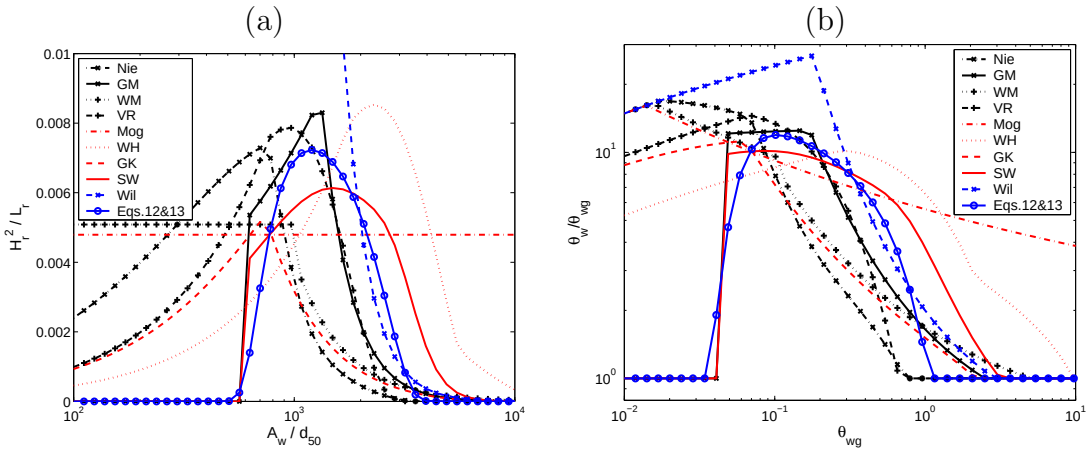

Figure 7: Ratio $H_r{}^2/L_r$ versus the ratio A_w/d_{50} (a) and the induced Shields parameter θ_w versus the ratio A_w/d_{50} (b) for a constant medium grain size $d_{50} = 0.25$ mm and a constant wave period $T_w = 6$ s using the different studied formulas for the ripple characteristics (the roughness height k_s was calculated using Eq. 17 with $a_r = 10$).

4.2 Influence of the ripple characteristics on the total Shields parameter

Using Eq. 17 with $a_r = 10$ for the calculation of the ripple-induced roughness height for the eight studied formulas, the total shear stress was estimated for the same conditions as in Fig. 7(a); *i.e.* with fixed median grain size and wave period. This condition is quite coherent with what is observed on a beach for a specific time: a large range of bed shear stresses with nearly constant median grain size and wave period. Fig. 7(b) shows a typical evolution of the ratio between the total and skin wave-related Shields parameters as a function of the skin wave-related Shields parameter using the different studied formulas.

For very small skin shear stress ($\theta_{wg} < \theta_{cr}$), as only the "GM" and "SW" formulas takes into account θ_{cr}, only these formulas yield realistic results. The other formulas predict a Shields parameter one order of magnitude larger than the skin Shields parameter. Even if there are some uncertainties in the prediction of the critical Shields parameter for the inception of movement (*cf.* Eq. 5), it is necessary to take into account this critical value.

For relatively small skin shear stresses ($\theta_{cr} < \theta_{wg} < 0.2$), most of the formulas present similar results which indicate a total Shields parameter approximately 5 to 10 times larger than the grain-related Shields parameter. It is possible to define an equilibrium value for the ratio between the total and the skin-related Shields parameters $(\theta_w/\theta_{wg})_{eq}$.

Then, for larger skin shear stress ($0.2 < \theta_{wg} < \theta_{cr,sf}$), the ratio θ_w/θ_{wg} is decreasing with an increasing skin-related Shields parameter. The ratio also appeared to be a decreasing function of d_{50} or T_w (suborbital regime). The uncertainties in the prediction of the ripples wash-out are very large. Even if Wiberg & Harris (1994)

observed that ripples cannot exist for $A_w/d_{50} > 6000$, most of the formulas, including the "WH" formula, yield a wash-out of the ripples ($\theta_w = \theta_{wg}$) for larger values of A_w/d_{50}. As no limit is provided, the "Mog" equation yields a presence of ripples whatever the shear stress, which is unrealistic. On the contrary, the "Nie" and "VR" formulas yield a wash-out of the ripples for $\theta_{wg} \approx 0.7 - 0.9$. This is more in agreement with the observations by Wiberg & Harris even if bed forms have been observed for higher shear stresses. An important parameter for the estimation the roughness height due to ripple is therefore the critical Shields parameter for the inception of sheet flow. It may also be observed that these formulas induce a nearly constant (even decreasing for the "VR" formula) total Shields parameter for an increasing wave orbital velocity when suborbital ripples are present ($1000 < A_w/d_{50} < 5000$).

It should be noted that f_w and then $(\theta_w/\theta_{wg})_{eq}$ are functions of the coefficient a_r (*cf.* Eq. 17) and strongly depend on the chosen value for a_r. Based on Kim (2004) numerical results, very different roughnesses are observed depending on the shape of the ripple. For sharp-crested ripples (pure oscillatory flow), $a_r = 13.4$ is obtained whereas using a sinusoidal profile with the same characteristics, $a_r \approx 6.3$ is obtained. In case of a wave and current interaction, where the shape of the ripples is much smoother, a relatively low coefficient should thus be used.

Soulsby & Whitehouse (2007**?**) proposed an alternative approach to compute the friction coefficient f_w using the drag coefficient approach on strip roughness elements :

$$f_w = \frac{M_{cd}}{A_w}\frac{{H_r}^2}{L_r} \tag{18}$$

with M_{cd} a coefficient (Soulsby & Whitehouse suggested to used $M_{cd} = 5$). In Fig. 8, the friction coefficient is plotted versus the ratio $({H_r}^2/L_r)/A_w$ with observed values from experiments of Jonsson & Carlsen (1976), and Mathisen & Madsen (1996) and numerical model results of Andersen (2001) and Kim (2004). Eq. 16 with Eq. 17 and Eq. 18 yield similar results when $f_w > 0.05$ and $M_{cd} \approx a_r/2$. From the observed values, it may be noted that a_r (M_{cd}) may vary from 5 to 30 (2.5 to 15). In the same way, $(\theta_w/\theta_{wg})_{eq}$ may vary by a factor 6 depending on the choice of a_r (or M_{cd}).

4.3 Estimation of the total Shields parameter directly from the skin Shields parameter

Following the observations in section 4.2 (and the trends of the empirical formulas in Fig. 7, as well as the study of ripple characteristics proposed in section 3.2) and using θ_{cr} (Eq. 5) and $\theta_{cr,sf}$ (Eq. 8), a simple formula is proposed to estimate the total Shields parameter due to the ripples directly from the grain-related Shields parameter:

$$\frac{\theta_w}{\theta_{wg}} = 1 + \left[\left(\frac{\theta_w}{\theta_{wg}}\right)_{eq} - 1\right] f_2\left(\frac{\theta_{cr}}{\theta_{wg}}\right) f_2\left(\frac{\theta_{wg}}{\theta_{cr,sf}}\right) \tag{19}$$

Author-produced version of the article published in Estuarine Coastal and Shelf Science,
vol. 84, n° 4, p. 553-564, doi : 10.1016/j.ecss.2009.07.022

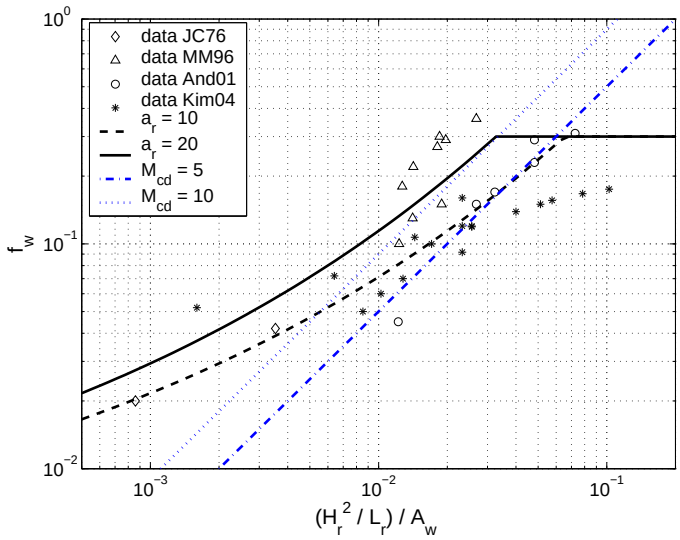

Figure 8: Wave related friction coefficient f_w as a function of the ratio $\left({H_r}^2/L_r\right)/A_w$ (Eq. 16 and Eq. 18 are plotted, using Eq. 17 with $a_r = 10$ and 20, and $M_{cd} = 5$ and 10, respectively, together with experimental data from Jonsson & Carlsen, 1976, and Mathisen & Madsen, 1996, and numerical data from Andersen, 2001, and Kim, 2004).

where the function f_2 was found to be $f_2(x) = f^2(x) = \exp(-2\alpha_{cr}x^4)$, and an estimation of the equilibrium value of the ratio θ_w/θ_{wg} may be:

$$\left(\frac{\theta_w}{\theta_{wg}}\right)_{eq} = 1 + 1.0\ a_r \exp\left(-1.5 \times 10^{-6}\ \frac{\theta_{wg}}{\chi}\right) \tag{20}$$

Using Eqs. 17 (with $a_r = 10$), 5, 8, 9 and 10, it is possible to estimate the total Shields parameter as a function of the skin Shields parameter. Fig. 9 presents a comparison between the method based on the ripple characteristics (1) and the empirical equation directly based on the skin Shields parameter (2: Eqs. 19 and 20). One can observe that both methods present very similar results. A truncation may appear using the first method for large grain size or wave period values combine with a large a_r-value as f_w reaches its maximum ($\max(f_w) = 0.3$, *cf.* Eq. 16). For fine sediments or short wave periods, the behaviour is similar to the Van Rijn formula, *i.e.* for $0.5 < \theta_{wg} < 1$ (*cf.* Fig. 7(b)), the total Shields parameter is a fast decreasing function of the grain-related Shields parameter, thus a decreasing function of the wave height, which needs to be validated. For coarser sediments or longer wave periods (*i.e.* for larger values of $\theta_{cr,sf}$), this effect is not as strong.

4.4 Comparison with data

Tab. 5 presents the statistical results on the prediction of the total Shields parameter using the different formulas for the prediction of ripple characteristics. As for the previous calculations, Eq. 17 with $a_r = 10$ was used to estimate the ripple-induced roughness height for both measured and estimated data. It appeared logically that the formulas which predict the best ripple characteristics yield the most

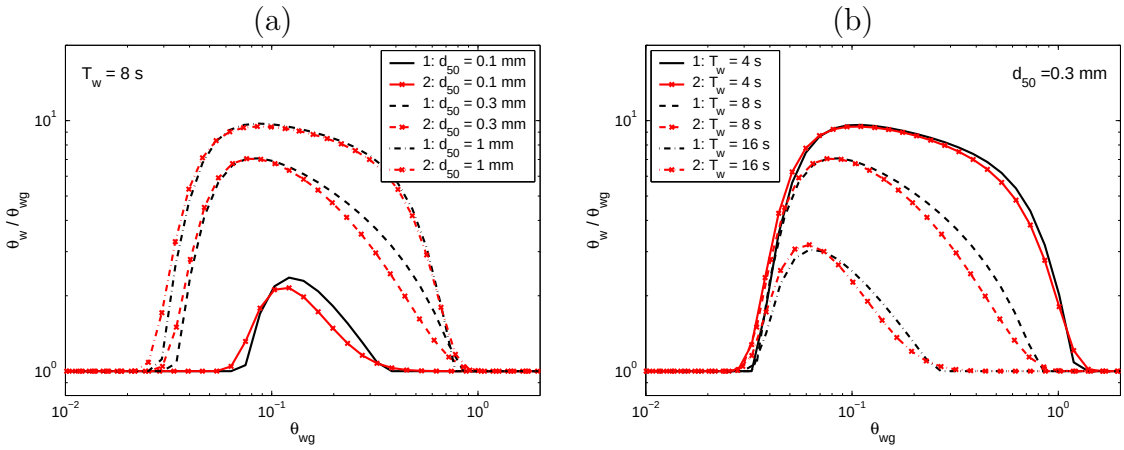

Figure 9: Total Shields parameter versus the skin Shields for several median grain sizes (a) and wave periods (b) using the classical method based on the prediction of the ripple characteristics (1: black lines) or Eq. 19 (2: red lines with crosses).

accurate predictions of the total Shields parameter. Thereby, the Van Rijn, Soulsby & Whitehouse formulas as well as the suggested formula (Eqs. 9 and 10) yield the best results. Using $\alpha_{cr} = 1$ does influence the results as the Shields parameter is strongly underestimated when $\theta_{wg} < \theta_{cr}$ whereas ripples were observed. In the same way, Eq. 19, which estimated the total Shields parameter directly from the skin Shields parameter, yields satisfactory results although it may underestimate results for $\theta_{wg} < \theta_{cr}$ or $\theta_{wg} > \theta_{cr,sf}$. On the other hand, much better results are observed for the data set where ripples are washed out.

Table 5: Prediction of the Shields parameter from the estimation of the ripple characteristics using various empirical equations and the collected experimental data.

	ripple data				data for $\theta_w = \theta_{cr,sf}$			
Equation	$P1.2$	$P2$	μ_f	σ_f	$P1.2$	$P2$	μ_f	σ_f
Nielsen	19%	48%	−0.24	0.42	85%	96%	+0.04	0.10
Grant & Madsen	16%	53%	−0.02	0.45	17%	46%	+0.36	0.26
Wikramanayake & Madsen	15%	52%	−0.14	0.40	10%	38%	+0.58	0.38
Van Rijn	29%	64%	+0.005	0.40	39%	59%	+0.27	0.28
Mogridge *et al.*	13%	43%	+0.51	0.48	0%	14%	+0.47	0.16
Wiberg & Harris	18%	62%	+0.09	0.35	0%	0%	+0.83	0.14
Grasmeijer & Kleinhans	10%	50%	−0.15	0.39	15%	82%	+0.20	0.12
Soulsby & Whitehouse	25%	73%	+0.02	0.33	0%	0%	+0.85	0.11
Eqs. 9 and 10, $\alpha_{cr} = 0.01$	36%	78%	−0.05	0.30	4%	5%	+0.79	0.22
Eqs. 9 and 10, $\alpha_{cr} = 1$	34%	74%	−0.11	0.33	46%	58%	+0.29	0.31
Eq. 19	32%	71%	−0.12	0.36	30%	45%	+0.41	0.36

In Fig. 10, it clearly appears that the underestimation is mainly due to the error on the estimation of the critical Shields parameters. Indeed, the formulas induce an

Author-produced version of the article published in Estuarine Coastal and Shelf Science,
vol. 84, n° 4, p. 553-564, doi : 10.1016/j.ecss.2009.07.022

underestimation of the results when $\theta_{wg} < \theta_{cr}$ or $\theta_{wg} > \theta_{cr,sf}$, where θ_{cr} and $\theta_{cr,sf}$ are estimated values.

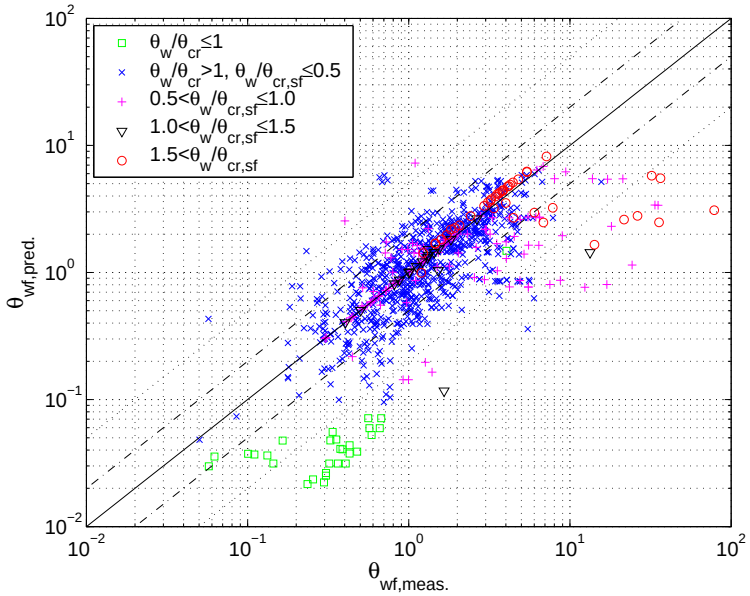

Figure 10: Prediction of the Shields parameter using Eq. 17 with $a_r = 20$ for the estimation of the roughness and the observed and estimated (Eqs. 9 and 10 with $\alpha_{cr} = 1$) characteristics of the ripples.

5 Conclusion

From this sensitivity analysis, it appears that large scatters exist in the prediction of ripple characteristics and so on the ripple-related roughness depending on the formulas applied. One important point to be considered is the critical Shields parameters for the inception of sediment movement θ_{cr} and for the inception of sheet flow $\theta_{cr,sf}$, which should border the limits for the existence of ripples. Only the Grant & Madsen and Soulsby & Whitehouse formulas take into account θ_{cr} and only the Nielsen and Van Rijn formulas include the sheet flow limit, even if both formulas seem to underestimate the wash-out of the ripples. Thus, even if the Soulsby & Whitehouse formula yields the best prediction for the ripple characteristics and induced Shields parameter, it does not take into account properly the inception of sheet flow and largely overestimates the results when ripples are washed out.

A new set of formulas (Eqs. 9 to 13) for ripple characteristics was proposed based on these two critical Shields parameters. The ripple steepness H_r/L_r and dimensionless ripple length L_r/A_w were found to reach an equilibrium value as soon as $\theta_c < \theta_{wg} < \theta_{cr,sf}$ where $\theta_{cr,sf}$ is estimated based on Camenen & Larson (2006) study. For the ripple steepness H_r/L_r, this equilibrium value appeared to be nearly constant and equal to 0.16. For the dimensionless ripple length L_r/A_w, it has been found to be a decreasing function of χ and θ_{wg}.

Author-produced version of the article published in Estuarine Coastal and Shelf Science,
vol. 84, n° 4, p. 553-564, doi : 10.1016/j.ecss.2009.07.022

It should be noted that this set of formulas does not take into account relict ripples. As suggested by Soulsby & Whitehouse (2007**?**), it could be partly taken into account assuming ripples take pre-existing values of H_r and L_r when $\theta_w < \theta_{cr}$. However, the hysteresis effect due to relict ripples as observed by Traykovski *et al.* (1999) appears to be much more difficult to model, especially when there is a reorganisation from 2D to 3D wave ripples.

A discussion is also proposed to explain the differences observed for the case of large wave ripples (LWR). The effect of an additional current appeared not to be so significant for the prediction of ripple characteristics. However, it should strongly affect the induced roughness by smoothing the ripples and making the ripple system 3D.

The importance of the critical Shields parameter appeared to be even more significant when calculating the total Shields parameter. The roughness height for a rippled bed was also found to be as sensitive to the parameter a_r (which varies from 8 to 37.5 depending on the authors) as to the ripple height and length. One future challenge would be to properly estimate the coefficient a_r depending on the shape of the ripples, and so on the ratio $|U_c|/U_w$, using both experimental data and numerical tests.

All the uncertainties to estimate these parameters might explain the large scattering observed in many results for the estimation of the sediment transport. A simple empirical formula (Eq. 19) was then suggested to estimate the total Shields parameter in the ripple regime directly from the grain-related Shields parameter. The excess shear stress is proportional to a_r and a decreasing function of the ratio θ_{wg}/χ. The proposed formula yields satisfactory results compared to the classical methods based on ripple characteristics.

Acknowledgment

This work was conducted under the Inlet Modeling System Work Unit of the Coastal Inlets Research Program, U.S. Army Corps of Engineers, and partly sponsored by the Japanese Society for the Promotion of Science. I also would like to thanks R.L. Soulsby for for his very helpful comments, suggestions, and corrections.

References

Andersen, K. (2001), The dissipation of waves over a rippled bed, *in* L. Van Rijn, A. Davies, J. Van der Graff & J. Ribberink, eds, 'SEDMOC: Sediment transport Modelling in Marine Coastal Environments', Aqua Publications, The Netherlands, chapter AL.

Bagnold, R. (1946), 'Motion of waves in shallow water: interaction between waves and sand bottom', *Proc. Royal Society of London* **A**(187), 1–15.

Bosman, J. (1982), Concentration distribution under waves and current, Technical Report M 1875, Coastal Eng. Dpt., Delft Univ. of Technology, Delft, The Netherlands. (in Dutch).

Camenen, B. & Larson, M. (2006), 'Phase-lag effects in sheet flow transport', *Coastal Eng.* **53**, 531–542.

Camenen, B. & Larson, M. (2008), 'A suspended load sediment transport formula for the nearshore', *J. Coastal Res.* **24**(3), 615–627.

Catano-Lopera, Y. & Garcia, M. (2006*a*), 'Geometry and migration characteristics of bedforms under waves and currents. part 1: Sandwave morphodynamics', *Coastal Eng.* **53**, 767–780.

Catano-Lopera, Y. & Garcia, M. (2006*b*), 'Geometry and migration characteristics of bedforms under waves and currents. part 2: Ripples superimposed on sandwaves', *Coastal Eng.* **53**, 781–792.

Delgado Blanco, M., Bell, P. & Montaliu, J. (2004), A new look to the applicability of classical models for ripple prediction, *in* 'Proc. 29th Int. Conf. Coastal Eng.', ASCE, Lisbon, Portugal, pp. 1909–1921.

Dingler, J. (1974), Wave formed ripples in nearshore sands, PhD thesis, University of California, San Diego, California, USA.

Doucette, J. (2000), 'The distribution of nearshore bedforms and effects on sand suspension on low-energy, micro-tidal beaches in southwestern australia', *Marine Geology* **165**, 41–61.

Doucette, J. (2002), 'Geometry and grain-size sorting of ripples on low-energy sandy beaches: field observations and model predictions', *Sedimentology* **49**, 483–503.

Faraci, C. & Foti, E. (2002), 'Geometry, migration and evolution of small-scale bedforms generated by regular and irregular waves', *Coastal Eng.* **47**, 35–52.

Grant, W. & Madsen, O. (1982), 'Movable bed roughness in unsteady oscillatory flow', *J. Geophysical Res.* **87**(C1), 469–481.

Grasmeijer, B. & Kleinhans, M. (2004), 'Observed and predicted bed forms and their effect on suspended sand concentrations', *Coastal Eng.* **51**, 351–371.

Grasmeijer, B. & Van Rijn, L. (1999), 'Transport of fine sands by currents and waves (iii)', *J. Waterways, Port, Coastal & Ocean Eng.* **125**(2), 71–79.

Hanes, D., Alymov, V. & Chang, Y. (2001), 'Wave-formed ripples at Duck, North Carolina', *J. Geophysical Res.* **106**(C10), 22575–22592.

Hanson, H. & Camenen, B. (2007), Closed form solution for threshold velocity for initiation of sediment motion under waves, *in* 'Proc. Coastal Sediments'07', ASCE, New Orleans, Louisiana, USA, pp. 15–28.

Hume, T., Green, M. & Oldman, J. (1999), What happens at the seabed of a headland during tropical cyclone?, *in* 'Proc. Coastal Sediments'99', ASCE, Long Island, New York, USA, pp. 1836–1851.

Inman, D. (1957), Wave generated ripples in nearshore sands, Technical Report Tech. Memo. 100, Beach Erosion Board, US Army Corps of Engineers.

Jonsson, I. & Carlsen, N. (1976), 'Experimental and theoretical investigations in a oscillatory turbulent boundary layer', *J. Hydraulic Res.* **14**, 45–60.

Khelifa, A. & Ouellet, Y. (2000), 'Prediction of sand ripple geometry under waves and current', *J. Waterways, Port, Coastal & Ocean Eng.* **126**(1), 14–22.

Kim, H. (2004), 'Effective form roughness of ripples for waves', *J. Coastal Res.* **20**(3), 731–738.

Kleinhans, M. (2005), Phase diagram of bed states in steady, unsteady , oscillatory and mixed flows, *in* L. Van Rijn, R. Soulsby, P. Hoekstra & A. Davies, eds, 'SANDPIT: Sand Transport and Morphology of Offshore Sand Mining Pits', Aqua Publications, The Netherlands, chapter Q.

Lofquist, K. (1978), Sand ripple growth in an oscillatory-flow water tunnel, Technical Report TP-78-5, Coastal Engineering Research Center, U.S. Army Corps of Engineers. 101 pp.

Malarkey, J. & Davies, A. (2003), 'A non-iterative procedure for the wiberg and harris (1994) oscillatory sand ripple predictor', *J. Coastal Res.* **19**(3), 738–739.

Mathisen, P. & Madsen, O. (1996), 'Waves and currents over a fixed ripples bed. 1. bottom roughness experienced by waves in the presence and absence of currents', *J. Geophysical Res.* **101**(C7), 16533–16542.

Miller, R. & Komar, P. (1980), 'A field investigation of the relationship between ripple spacing and near bottom water motions', *J. Sedimentary Petrology* **50**(1), 183–191.

Mogridge, G., Davies, M. & Willis, D. (1994), 'Geometry prediction for wave-generated bedforms', *Coastal Eng.* **22**, 255–286.

Nielsen, P. (1981), 'Dynamics and geometry of wave generated ripples', *J. Geophysical Res.* **86**(C7), 6467–6472.

Nielsen, P. (1984), 'Field measurements of time-averaged suspended sediment concentrations under waves', *Coastal Eng.* **8**, 51–72.

Nielsen, P. (1992), *Coastal bottom boundary layers and sediment transport*, Vol. 4 of *Advanced Series on Ocean Engineering*, World Scientific Publication, Singapore.

O'Donoghue, T. & Clubb, G. (2001), 'Sand ripples generated by regular oscillatory flow', *Coastal Eng.* **44**, 101–115.

O'Donoghue, T., Doucette, J., Van der Werf, J. & Ribberink, J. (2005), Flow tunnel measurements of full-scale ripples in oscillatory flow, *in* L. Van Rijn, R. Soulsby, P. Hoekstra & A. Davies, eds, 'SANDPIT: Sans Transport and Morphology of Offshore Mining Pits', Aqua Publications, chapter V.

Ribberink, J. & Al Salem, A. (1994), 'Sediment transport in oscillatory boundary layers in cases of rippled beds and sheet flow', *J. Geophysical Res.* **99**(C6), 707–727.

Sato, S. (1987), Oscillatory boundary layer flow and sand movement over ripples, PhD thesis, University of Tokyo, Tokyo, Japan.

Sleath, J. (1982), 'The suspension of sand by waves', *J. Hydraulic Res.* **20**(5), 439–451.

Sleath, J. & Wallbridge, S. (2002), 'Pickup from ripples beds in oscillatory flow', *J. Waterways, Port, Coastal & Ocean Eng.* **128**(6), 228–237.

Soulsby, R. (1997), *Dynamics of marine sands, a manual for practical applications*, Thomas Telford, London, UK. ISBN 0-7277-2584.

Soulsby, R. & Whitehouse, R. (1997), Threshold of sediment motion in coastal environment, *in* 'Proc. Pacific Coasts and Ports'97 Conf.', University of Canterbury, Christchurch, New Zealand, pp. 149–154.

Soulsby, R. & Whitehouse, R. (2005*a*), Prediction of ripple properties in shelf seas: Mark 1, predictor, Technical Report TR 150, HR Wallingford, Wallingford, UK.

Soulsby, R. & Whitehouse, R. (2005*b*), Prediction of ripple properties in shelf seas: Mark 2, predictor for time evolution, Technical Report TR 154, HR Wallingford, Wallingford, UK.

Steetzel, H. (1985), Model tests of scour near the toe of dune revetments, Technical Report M 2051-II, Coastal Eng. Dpt., Delft Univ. of Technology, Delft, The Netherlands. (in Dutch).

Swart, D. (1974), Offshore sediment transport and equilibrium beach profiles, Technical report, Delft Hydraulics Lab. Publ., Delft, The Netherlands.

Traykovski, P., Hay, A., Irish, J. & Lynch, J. (1999), 'Geometry, migration, and evolution of wave orbital ripples at leo-15', *J. Geophysical Res.* **104**(C1), 1505–1524.

Van der Werf, J. & Ribberink, J. (2004), Wave induced sediment transport processes in the ripple regime, *in* 'Proc. 29th Int. Conf. Coastal Eng.', ASCE, Lisbon, Portugal, pp. 1741–1753.

Van der Werf, J., Ribberink, J., O'Donoghue, T. & Doucette, J. (2006), 'Modelling and measurement of sand transport processes over full-scale ripples in oscillatory flow', *Coastal Eng.* **53**, 657–673.

Van Rijn, L. (1993), *Principles of sediment transport in rivers, estuaries and coastal seas*, Aqua Publications, The Netherlands.

Van Rijn, L. (2007), 'Unified view of sediment transport by currents and waves. I: Initiation of motion, bed roughness, and bed-load transport', *J. Hydraulic Eng.* **133**(6), 649–667.

Van Rijn, L., Davies, A., Van der Graff, J. & Ribberink, J., eds (2001), *Sedmoc: Sediment Transport Modelling in Marine Coastal Environments*, Aqua Publications, Amsterdam, The Netherlands. ISBN 90-800346-4-5.

Van Rijn, L. & Havinga, F. (1995), 'Transport of fine sands by currents and waves (II)', *J. Waterways, Port, Coastal & Ocean Eng.* **121**(2), 123–143.

Van Rijn, L., Nieuwjaar, M., Van der Kaay, T., Nap, E. & Van Kampen, A. (1993), 'Transport of fine sands by currents and waves (I)', *J. Waterways, Port, Coastal & Ocean Eng.* **119**(2), 123–143.

Wiberg, P. & Harris, C. (1994), 'Ripple geometry in wave-dominated environments', *J. Geophysical Res.* **99**(C1), 775–789.

Wikramanayake, P. & Madsen, O. (1991), Calculation of movable bed friction factors, Technical report, Massachusetts Inst. of Tech., Cambridge, Massachusetts. 105 pp.

Williams, J., Bell, P. & Thorne, P. (2005), 'Unifying large and small wave-generated ripples', *J. Geophysical Res.* **110**(C2008), 1–18.

Williams, J., Bell, P., Thorne, P., Metje, N. & Coates, L. (2004), 'Measurement and prediction of wave-generated suborbital ripples', *J. Geophysical Res.* **109**(C2004), 1–18.

Wilson, K. (1989), 'Friction of wave induced sheet flow', *Coastal Eng.* **12**, 371–379.

Appendix: Predictive equations for ripples characteristics

Nielsen formula (1981)

Nielsen (1981) proposed the following equation for the ripple wave length based on the field data of Inman (1957), Dingler (1974), and Miller & Komar (1980):

$$L_r = \exp\left(\frac{693 - 0.37\ \ln^8 \Psi_w}{1000 + 0.75\ \ln^7 \Psi_w}\right)\ A_w \tag{21}$$

Using the data by Inman (1957) and Dingler (1974), Nielsen (1981) observed a wash-out of the ripples for a skin Shields number $\theta_{ws} \approx 0.8 - 1$. The maximum ripple steepness also appeared larger for irregular waves ($\max(H_r/L_r) \approx 0.35$) than regular waves ($\max(H_r/L_r) \approx 0.20$). Nielsen proposed an equation for the ripple steepness in case of irregular waves:

$$\frac{H_r}{L_r} = 0.342 - 0.34\ {\theta_{wg}}^{0.25} \tag{22}$$

Grant & Madsen formula (1982)

Grant & Madsen (1982) presented a set of empirical equations for the prediction of ripple characteristics. They distinguished a break-off point (critical Shields parameter) below/above which the ripple steepness is increasing/decreasing:

$$\theta_B = 1.8\theta_{cr}\ \left(\frac{{d_*}^{1.5}}{4}\right)^{0.6} \tag{23}$$

They proposed the following relationships functions of the skin wave-related Shields parameter:

$$\frac{H_r}{A_w} = \begin{cases} 0.22\ \left(\dfrac{\theta_{wg}}{\theta_{cr}}\right)^{-0.16} & \text{for } \theta_{cr} < \theta_{wg} \leq \theta_B \\ 0.48 \left(\dfrac{{d_*}^{1.5}}{4}\right)^{0.8}\ \left(\dfrac{\theta_{wg}}{\theta_{cr}}\right)^{-1.5} & \text{for } \theta_B < \theta_{wg} \end{cases} \tag{24}$$

$$\frac{H_r}{L_r} = \begin{cases} 0.16\ \left(\dfrac{\theta_{wg}}{\theta_{cr}}\right)^{-0.04} & \text{for } \theta_{cr} < \theta_{wg} \leq \theta_B \\ 0.28 \left(\dfrac{{d_*}^{1.5}}{4}\right)^{0.6}\ \left(\dfrac{\theta_{wg}}{\theta_{cr}}\right)^{-1.0} & \text{for } \theta_B < \theta_{wg} \end{cases} \tag{25}$$

Van Rijn formula (1993)

Van Rijn (1993) proposed the following relationships for the wave ripples in case of irregular waves and as functions of the mobility parameter Ψ_w:

$$\frac{H_r}{A_w} = \begin{cases} 0.22 & \text{for } \Psi_w \leq 10 \\ 2.8 \times 10^{-13}(250 - \Psi_w)^5 & \text{for } 10 < \Psi_w \leq 250 \end{cases} \tag{26}$$

$$\frac{H_r}{L_r} = \begin{cases} 0.18 & \text{for } \Psi_w \leq 10 \\ 2.0 \times 10^{-7}(250 - \Psi_w)^{2.5} & \text{for } 10 < \Psi_w \leq 250 \end{cases} \tag{27}$$

Wikramanayake & Madsen formula (1991)

Wikramanayake & Madsen (1991) proposed a relationship using that the ratio of the mobility number Ψ_w to the non dimensional sediment parameter S_*:

$$S_* = \frac{d_{50}}{4\nu}\sqrt{(s-1)gd_{50}} \tag{28}$$

For irregular waves, they chose U_{rms} to represent the wave orbital velocity U_w (Assuming a Rayleigh distribution, $U_{rms} = 1/\sqrt{2}U_{1/3}$). They found a good correlation with the field ripple data of Inman (1957), Dingler (1974) and Nielsen (1984) using the following equations:

$$\frac{H_r}{A_w} = \begin{cases} 0.27 \left(\dfrac{\Psi_w}{S_*}\right)^{-0.5} & \text{for } \dfrac{\Psi_w}{S_*} \leq 3.0 \\ 0.52 \left(\dfrac{\Psi_w}{S_*}\right)^{-1.1} & \text{for } \dfrac{\Psi_w}{S_*} > 3.0 \end{cases} \tag{29}$$

$$\frac{L_r}{A_w} = \begin{cases} 1.70 \left(\dfrac{\Psi_w}{S_*}\right)^{-0.5} & \text{for } \dfrac{\Psi_w}{S_*} \leq 3.0 \\ 2.10 \left(\dfrac{\Psi_w}{S_*}\right)^{-0.7} & \text{for } \dfrac{\Psi_w}{S_*} > 3.0 \end{cases} \tag{30}$$

It should be noted that the coefficients have been modified as Wikramanayake & Madsen (1991) based their results on the root-mean-square value of the wave excursion. Moreover, when $\Psi_w/S_* \leq 4.2$, the ripple height and wave length are only functions of the sediment characteristics.

Mogridge *et al.* formula (1994)

Mogridge *et al.* (1994) conducted an extensive study on previously published experimental data in both laboratory and field. They found some complex empirical relationships based on the wave period parameter χ. The complexity of the formula makes it however difficult to use. A simplified version is as following:

$$\frac{L_r}{d_{50}} = \min\left(10^{3.373-13.772\chi^{0.02054}}, 1394\right) \tag{31}$$

$$\frac{H_r}{d_{50}} = 10^{8.542-10.822\chi^{0.03967}} \tag{32}$$

On a real case, the wave period and median grain size do not vary significantly along a cross-shore beach profile whereas ripple characteristics do vary a lot (from well formed ripples offshore to a flat bed in the surf zone as ripples are washed-out).

Wiberg & Harris formula (1994)

Wiberg & Harris (1994) proposed iterative formulas for the prediction of the ripple characteristics which is also difficult to use. However, Malarkey & Davies (2003) proposed a simplified procedure to avoid the iterative calculation. The ripple characteristics read:

$$L_r = \begin{cases} 0.62A_w & \text{for } AH < 20 \\ 535d_{50} \exp\left[-\ln\left(\dfrac{0.62A_w}{535d_{50}}\right) \dfrac{\ln(0.01AH)}{\ln 5}\right] & \text{for } 20 \leq AH \leq 100 \\ 535d_{50} & \text{for } AH > 100 \end{cases} \tag{33}$$

Author-produced version of the article published in Estuarine Coastal and Shelf Science,
vol. 84, n° 4, p. 553-564, doi : 10.1016/j.ecss.2009.07.022

with $AH = A_w/H_{r,ano}$ where $H_{r,ano}$ is the anorbital ripple height calculated using the following equation for the ripple height with $L_r = 535 d_{50}$:

$$\frac{A_w}{H_r} = \exp\left[C_1 - \sqrt{C_2 - C_3 \ln\left(\frac{A_w}{L_r}\right)}\right] \tag{34}$$

with $C_1 = 7.59$, $C_2 = 33.60$ and $C_3 = 10.53$.

Grasmeijer & Kleinhans formula (2004)

More recently, Grasmeijer & Kleinhans (2004) proposed some equations based on the Nielsen (1981) study. They fitted an empirical relationship using laboratory data by Van Rijn *et al.* (1993), Van Rijn & Havinga (1995) and Grasmeijer & Van Rijn (1999) and field data by Inman (1957), Hanes *et al.* (2001) as well as their own data set measured near the coast of Egmond aan Zee, The Netherlands:

$$\frac{H_r}{A_w} = \begin{cases} 0.275 - 0.022{\Psi_w}^{0.5} & \text{for } \Psi_w \leq 10 \\ 2{\Psi_w}^{-1} & \text{for } 10 < \Psi_w \end{cases} \tag{35}$$

$$\frac{H_r}{L_r} = \begin{cases} -0.078 + 0.355{\Psi_w}^{-0.221} & \text{for } \Psi_w \leq 10 \\ 0.14 & \text{for } 10 < \Psi_w \end{cases} \tag{36}$$

Soulsby & Whitehouse formula (2005)

Soulsby & Whitehouse (2005) proposed a new equation based on an extensive study and Wiberg & Hanes (1994) observations. Following findings of O'Donoghue *et al.* (2005), for irregular waves, they chose $U_{1/10}$, the mean of the highest one-tenth velocities to represent the wave orbital velocity U_w (Assuming a Rayleigh distribution, $U_{1/10} = 1.80 U_{rms} = 1.27 U_{1/3}$). In irregular waves, they assumed the peak-period T_p gives the best representation of T_w.

$$\frac{L_r}{A_w} = \left[1 + 1.87 \times 10^{-3} \frac{A_w}{d_{50}} \left(1 - \exp\left\{-\left(2.0 \times 10^{-4} \frac{A_w}{d_{50}}\right)^{1.5}\right\}\right)\right]^{-1} \tag{37}$$

$$\frac{H_r}{L_r} = 0.15 \left[1 - \exp\left\{-\left(5000 \frac{d_{50}}{A_w}\right)^{3.5}\right\}\right] \tag{38}$$

An additional constraint is that ripples can only form and evolve if the wave-induced stress exceeds the threshold of motion of the sediment, *i.e.* $\theta_{wg} > \theta_{cr}$.